

Simulation on deposition and solidification processes of 7075 Al alloy droplets in 3D printing technology

Hai-peng LI¹, He-jun LI¹, Le-hua QI², Jun LUO², Han-song ZUO¹

1. State Key Laboratory of Solidification Processing, Northwestern Polytechnical University, Xi'an 710072, China;
2. School of Mechatronics Engineering, Northwestern Polytechnical University, Xi'an 710072, China

Received 19 July 2013; accepted 5 November 2013

Abstract: In order to study the successive deposition and solidification processes of uniform alloy droplets during the drop-on-demand three dimensional (3D) printing method, based on the volume of fluid (VOF) method, a 3D numerical model was employed. In this model, the 7075 alloy with larger temperature range for phase change was used. The simulation results show that the successive deposition and solidification processes of uniform 7075 alloy droplets can be well characterized by this model. Simulated droplets shapes agree well with SEM images under the same condition. The effects of deposition and solidification of droplets result in vertical and L-shaped ridges on the surface of droplets, and tips of dendrites appear near the overlap of droplets due to rapid solidification.

Key words: 7075 Al alloy; uniform droplets; 3D model; 3D printing technology; surface morphology

1 Introduction

3D printing technology is an attractive alternative to the conventionally manufacturing techniques. As known as an additive technology, 3D printing technology has its exciting advantages in cost, speed and accuracy [1,2]. Among different types of methods of 3D printing technology, drop-on-demand (DOD) printing method is one of the advanced methods capable of forming 3D components [3–5]. In DOD printing method, individual droplets are ejected by a pressure wave only when needed and the processes of melting, molding, casting, solidification, and machining can be combined in a single process.

In DOD printing method, the deposition and solidification processes of droplets are important factors in the dimensional accuracy, mechanical properties, and surface quality of the components, especially for making polymer, micro-scale metal parts and electronic packaging [6]. However, it is difficult to directly observe the entire processes due to micro-scale droplets and the short time from a few to tens of microseconds.

Fortunately, changes of deposition and solidification processes can be predicated by means of numerical simulation.

Currently, a great deal of researches has been conducted on the deposition and solidification of lower melting point metal, alloy and liquid droplets on a substrate. For instance, QI et al [7] applied a novel selection method of scanning step and fabricated a three-dimensional Sn60–Pb40 component. CHAO et al [8] developed a direct droplet fabrication experiment system and fabricated a micro thin-walled structure of Sn60–Pb40. KANAI et al [9] investigated the wetting and reaction between Si droplet and SiO₂ substrate. LIANG et al [10] observed the phenomena of water droplet impact on solid surface with a pre-existing liquid film and analyzed the processes of droplet spreading, liquid sheet formation, splashing and droplet oscillation. CHEN et al [11] built a water droplet oscillation model and obtained the expression of the droplet spreading radius. LI et al [12] established a two-dimensional SPH model to investigate the process of water droplet impact on an orifice plate and numerical results were in good agreement with the experimental data. However, the

Foundation item: Projects (51005186, 51221001) supported by the National Natural Science Foundation of China; Project (85-TZ-2013) supported by the Research Fund of the State Key Laboratory of Solidification Processing (NWPU), China; Project (20126102110022) supported by the Doctoral Fund of Ministry of Education of China

Corresponding author: He-jun LI; Tel: +86-29-88495004; E-mail: lihejun@nwpu.edu.cn
DOI: 10.1016/S1003-6326(14)63261-1

studies on low melting point metal, alloy and liquid droplets cannot provide enough useful information for the practical application due to the manufacturing of components including high-melting point melt droplets. Thus, it is important to investigate the deposition and solidification processes of high-melting point metal droplets. TRAPAGA et al [13] studied heat transfer and solidification of a copper droplet impingement process, and compared simulated predictions with experimental results. The simulated results showed that spreading and solidification of large droplets with low impinging velocities appeared to take place at comparable rates. KUMAR et al [14] developed a numerical model for heat transfer during collision of a falling Al–33%Cu liquid droplet on a 304 stainless substrate. LI et al [15] established a 3D model based on a volume-of-fluid (VOF) method to investigate the successive deposition of molten Al droplets on a horizontally moving substrate, and found that the molten Al droplets solidified in a layer by layer mode due to the high heat conductivity. However, there is only just no or a small temperature range for the phase change of materials in these models, which makes it difficult to obtain enough useful knowledge for alloys droplets. Thus, investigation of a large temperature range for the phase change in the simulation is still necessary.

In the present work, the 3D numerical model proposed by LI et al [15] has been employed to high-melting point 7075 Al alloy as materials for simulation. Additionally, surface morphology of 7075 Al alloy droplets was studied.

2 Experimental

7075 Al alloy with a composition (mass fraction, %) of 5.1–6.1 Zn, 2.1–2.9 Mg, 1.2–2.0 Cu, 0.5 Fe, 0.4 Si, 0.4 Cr and 0.3 Mn, balance aluminum, was used for DOD printing method. As one of the most widely used aluminum alloys, 7075 Al alloy was originally developed as one kind of high strength alloys for manufacturing aircraft parts [16–18]. The thermo-physical properties of the 7075 Al alloy with a temperature range of 145.14 K for phase change are shown in Table 1. The generation of droplets in experiment was conducted. The alloy was heated to 975–1275 K and maintained for half an hour in a graphite crucible, then droplets were ejected out at a rate of 1 Hz through a nozzle in the bottom of the crucible by enabling pressure pulses to the liquid metal. Subsequently, the atomized droplets were deposited onto a horizontally moving Ni substrate under room temperature. Argon gas was used as protective gas in order to reduce the strong oxidation effect of 7075 Al alloy droplets.

Table 1 Properties of 7075 Al alloy used in simulation

Property	Symbol	Value
Density/(kg·m ⁻³)	ρ	2487.92
Dynamics viscosity/(Pa·s)	μ	1.37×10^{-3}
Surface tension coefficient/(N·m ⁻¹)	σ	0.9
Heat conductivity coefficient/ (W·m ⁻¹ ·K ⁻¹)	k_s k_l	161.98 82.86
Specific heat capacity/ (J·kg ⁻¹ ·K ⁻¹)	c_{ps} c_{pl}	1462.5 1280
Latent heat for solidification/(J·kg ⁻¹)	L	351053
Liquidus temperature/K	T_l	944.14
Solidus temperature/K	T_s	799
Static contact angle/(°)		90

s: solid; l: liquid

3 Mathematical modeling

The 3D model employed in this work was discussed in detail in elsewhere [15], and it gives a brief description here. Fluid flow in deposition and solidification processes of droplets is modeled by a finite volume method of the Navier–Stokes equations in a 3D system. The liquid is assumed to be incompressible and any effect of the ambient air on droplets deposition and solidification is neglected. In this model, the droplets generated at a fixed frequent have a uniform initial temperature distribution before the impingement, and radiation form heat transfer after the impingement is ignored.

The momentum equation, continuity equation and energy conservation equation are given as follows:

$$\frac{\partial(\rho \mathbf{u})}{\partial t} + \nabla(\rho \mathbf{u} \mathbf{u}) - \nabla \left[\mu (\nabla \mathbf{u} + \nabla \mathbf{u}^T) \right] + \nabla p = \mathbf{F} + \rho \mathbf{g} + S \quad (1)$$

$$\frac{\partial \rho}{\partial t} + \nabla \cdot (\rho \mathbf{u}) = 0 \quad (2)$$

$$\rho \left(\frac{\partial H}{\partial t} + \mathbf{u} \cdot \nabla H \right) = \nabla \cdot (k \nabla T_d) \quad (3)$$

where ρ , μ , \mathbf{u} , p , t , H , S and T_d are density, dynamics viscosity, local fluid velocity, pressure inside the deforming droplet, time, enthalpy, a temperature-dependent source and droplet temperature, respectively; \mathbf{g} represents gravitational force; \mathbf{F} is a volume force representing surface tension in the momentum equation; k is thermal conductivity and used to describe the heat transfer inside the droplet.

The volume of fluid model used for numerical simulation is shown in Fig. 1. In this model, 1.5 mm-diameter 7075 Al alloy droplets with a velocity of 0.8 m/s at 975 K impact onto a horizontally moving substrate (10 mm×2.6 mm×0.95 mm) with a velocity of 0.055 mm/s. The mesh is chosen to be uniform square grid of 0.05 mm side length spacing in 3D direction, which equals 1/30 of the droplet diameter. The fluid dynamic

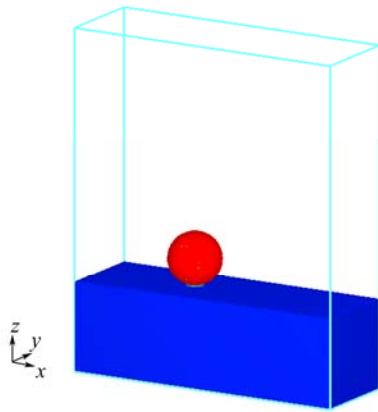


Fig. 1 Volume of fluid model

process during droplet spreading is determined by non-dimensional parameters, such as Weber number, Reynolds number and Ohnesorge number. The fluid flow is taken to be inviscid and impact-driven since the Weber number, Reynolds number and Ohnesorge number are estimated to be at most 2.67, 2179 and 0.00075, respectively, which means that the droplet is basically influenced by the dynamic pressure of impact and inertia after impact [19]. The commercial software Flow-3D 9.3 was used to implement the model described above.

4 Simulation results and discussion

4.1 Deposition of single droplet

Figure 2 shows the sequences of the numerical

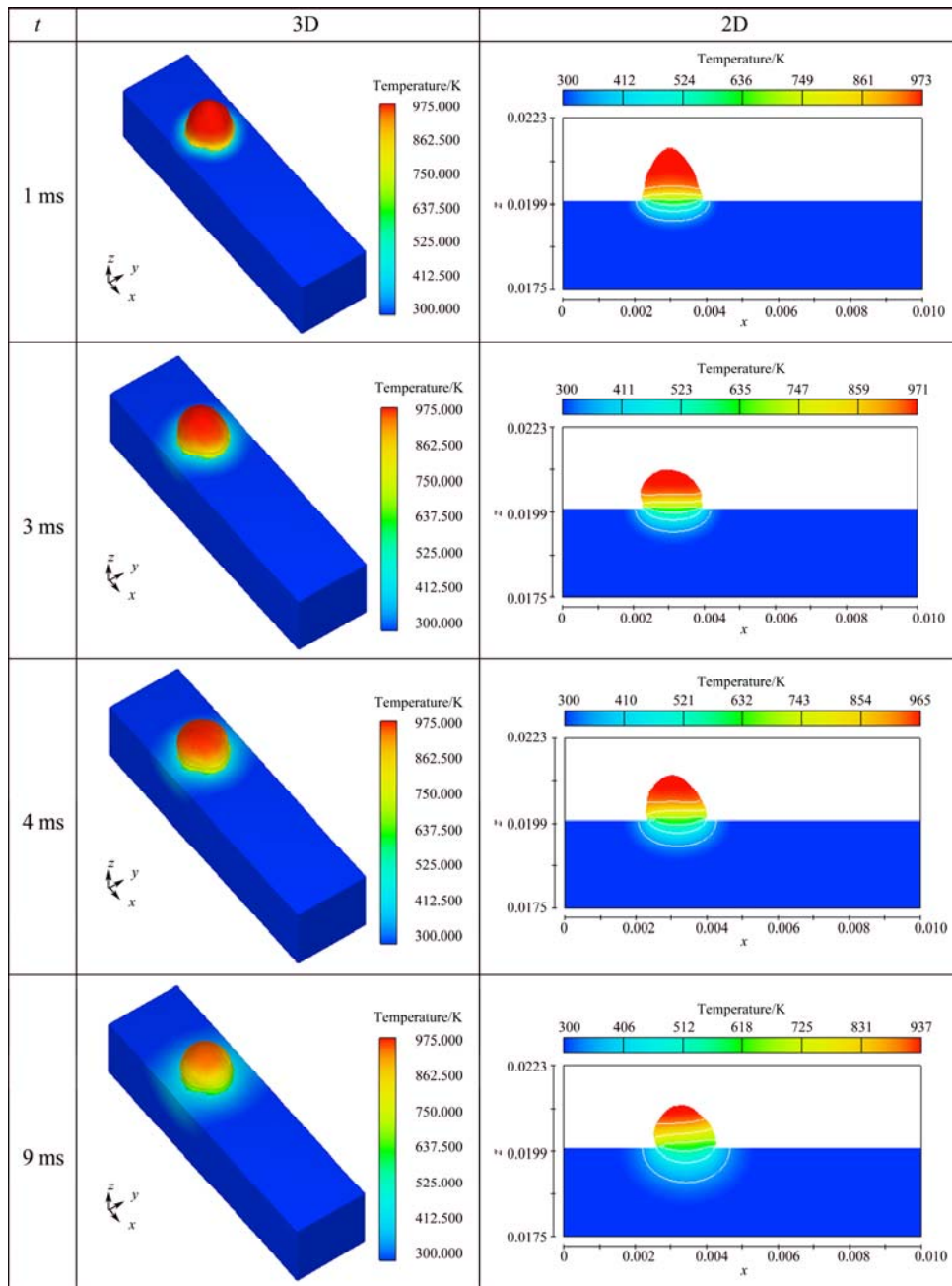


Fig. 2 Temperature distribution in 3D and corresponding temperature distribution in 2D of single droplet after impact

simulation of 7075 Al alloy droplet during successive stages of deposition and solidification and the cross section of the spreading droplet at the corresponding time. Immediately, after impact, the droplet was spread out in the radial direction and reached its maximum in a short time (at 3 ms). The rate of solidification was the fastest in the bottom region of the spreading droplet where it first contacted the colder substrate and the alloy began to solidify. Due to obstruction of flow made by the solidified layer around the splat bottom and surface tension which pulled back the liquid, the molten layer recoiled toward the top region of the splat (at 4 ms). Then when the molten layer lost its velocity upward due to the action of gravity and surface tension, it turned back and spread downward again. That is the cause of the formation of oscillation in the molten part of the droplet. Meanwhile, the solidification front advanced upward and the total heat loss was still going on. The effects of solicitation and solidification made a series of vertical ridges on the surface of the splat and ridges disappeared from the bottom region to the top region, as shown in Fig. 3. The size of vertical ridges and the spacing between them decreased from the bottom region to the top region. This phenomenon can be explained by the reductions of the initial droplet temperature and the initial impact velocity [20]. In addition, the top region of the droplet inclined slightly in the opposite direction of the movement of the substrate due to the effect of inertia, which could also be seen at 9 ms.

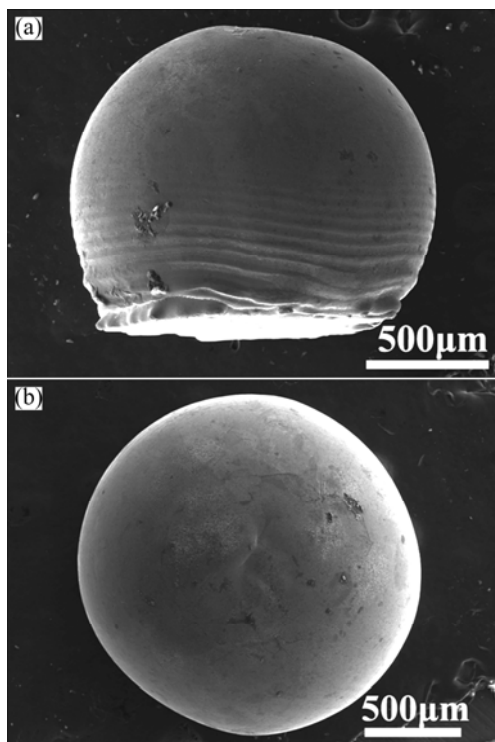


Fig. 3 SEM images of 1.5 mm diameter 7075 Al alloy droplet after solidification with velocity of 0.8 m/s at initial temperature of 975 K: (a) Front view; (b) Top view

4.2 Deposition of multiple droplets

Figure 4 shows sequences of the numerical simulation of the second 7075 Al alloy droplet during successive stages of impact, deposition and solidification, and the cross section of the spreading droplet at the corresponding time can be seen. After impact, the second droplet landed on the edge of the solidified droplet and then spread. Most of the second droplet freezes layer by layer fast in both planes paralleled to the interface, and the solidification front assumed L shape. The heat transferred from the high temperature droplet made part of the solidified droplet in the contact area remelt, which is beneficial to metallurgical bonding between droplets.

Figure 5 shows the computed images of droplets at 1 ms under different deposition orders. It is obviously observed that the second droplet excessively overlaps the first droplet, which can be attributed to the effect of the inclined top region of the first droplet during the deposition process. Apart from this, the processes of solidification and deposition of these four droplets are similar. These predicated droplets shapes, especially the last four droplets, well agree with SEM images of uniform molten 7075 Al alloy droplets onto a horizontally moving substrate under the same conditions (Fig. 6).

Figure 7 shows the temperature of each droplet at the top area with time during the deposition. It can be seen that the temperature decreases with the increase of time. Because of the solidification front rapidly moving to the top, the cooling rate of the tops increases after temperature falls below the liquidus, reaches the highest one around the solidus, and then decreases due to the release of solidification latent heat, where the cooling rate is derived from the temperature history curves. It is also observed that the cooling rates of the first droplet, the third droplet and the fourth droplet increase according to their order. This change in solidification can be attributed to the increase in heat dissipation area, which includes the solidified droplet and substrate for latter droplet. The temperature curve of the second droplet is abnormal due to extreme overlap with the first droplet, which would result in the rapid solidification for the second droplet.

5 Surface morphology

Figure 8 shows the SEM images of droplet surface in the bottom region of two droplets overlap. The bottom region of the droplets has a series of L-shaped ridges on its surface, as shown in Fig. 8(a), which can also be seen in the simulation results (Fig. 4). Meanwhile, tips of dendrites were observed in greater enlargement (Fig. 8(b)). The formation of tips of dendrites can be

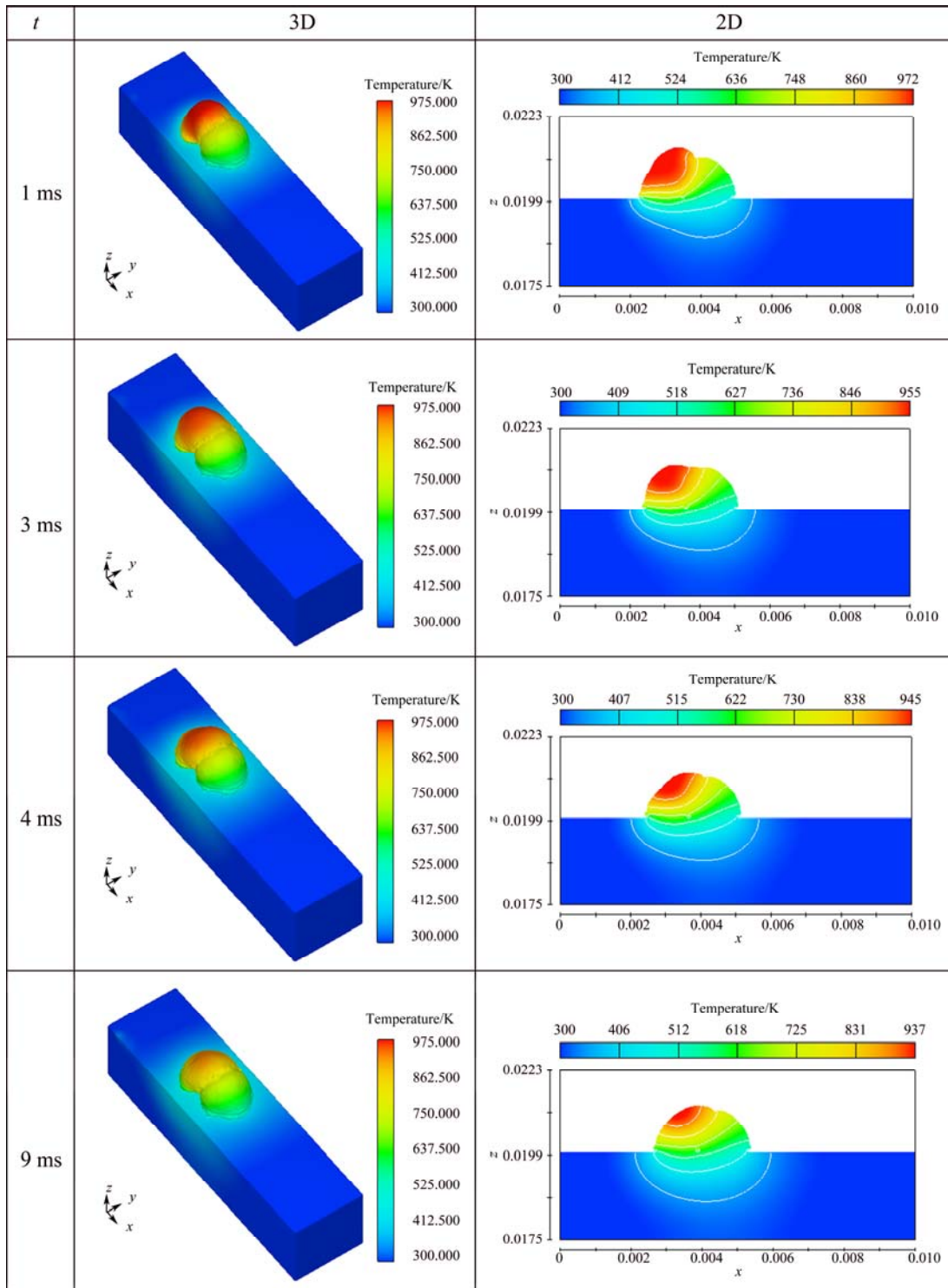


Fig. 4 Temperature distribution in 3D and corresponding temperature distribution in 2D of the second droplet after impact

attributed to the effect of surface tension and the compressive stress of solidification during the deposition. It can also be clear observed that the raised ridge is surrounded by valleys on both sides. This indicates that the oscillating liquid meets the solidification front, the spread part of the molten meat forms the raised ridge and the recoil part forms the valley (Fig. 8(c)). Figure 8(d) shows the surface morphology

between two ridges. It has a relatively flat surface compared with the area near the raised ridge.

Figure 9 shows the SEM images of droplet surface in the top region of two droplets overlap. The above droplet solidified earlier than the below droplet, and the below droplet initially impacted at interface between the above droplet and the substrate. It can be seen that small tips of dendrite form at the boundary between two

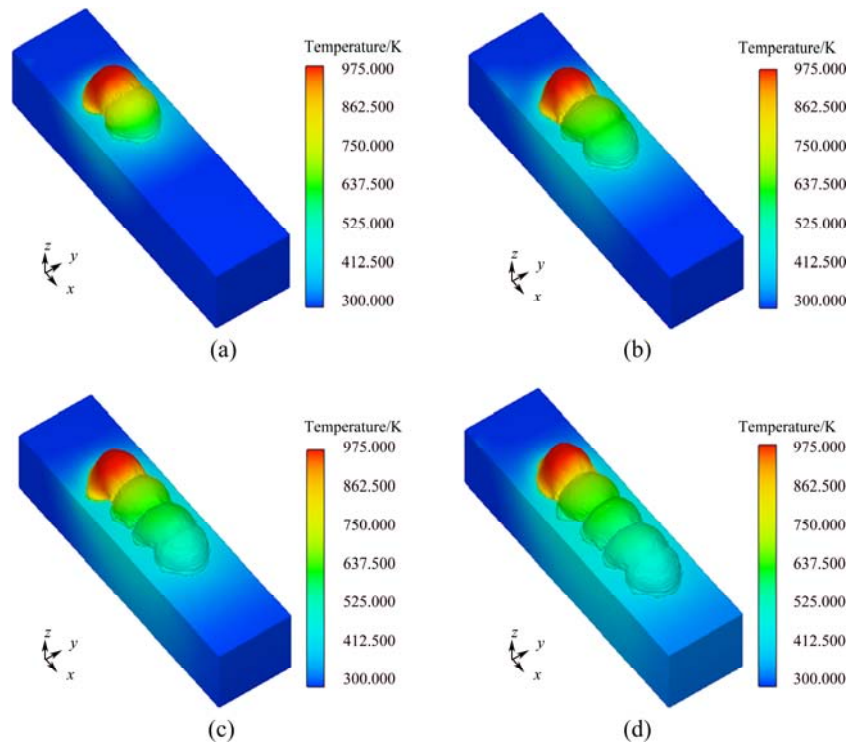


Fig. 5 Computed images of droplets after impact at 1 ms: (a) The second droplet; (b) The third droplet; (c) The fourth droplet; (d) The fifth droplet

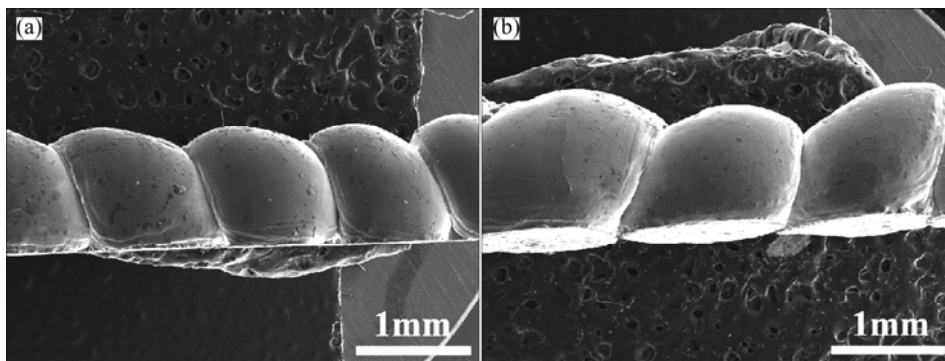


Fig. 6 SEM images of 1.5 mm diameter 7075 Al alloy droplets after solidification at different deposition stages: (a) Stable stage; (b) Initial stage with velocity of 0.8 m/s at initial temperature of 975 K

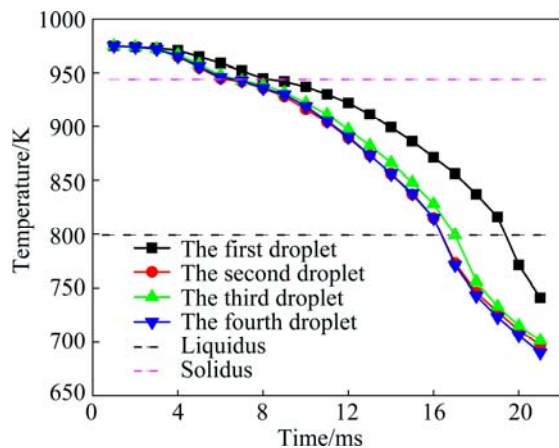


Fig. 7 Evolution of temperature of each droplet at top area during deposition

droplets, and droplet surface on each side of the boundary shows different morphology (Fig. 9(b)). Uniform tips of dendrites appear around the boundary on the below droplet due to rapid solidification occurring (Fig. 9(c)). Scaly tips of dendrites appear on the above droplet for this part metal remelting (Fig. 9(d)).

6 Conclusions

1) Mathematical model of the deposition and solidification of 7075 Al alloy uniform droplets is developed, and this model includes larger temperature range for phase change. The successive deposition and solidification processes of 7075 alloy droplets could be well characterized.

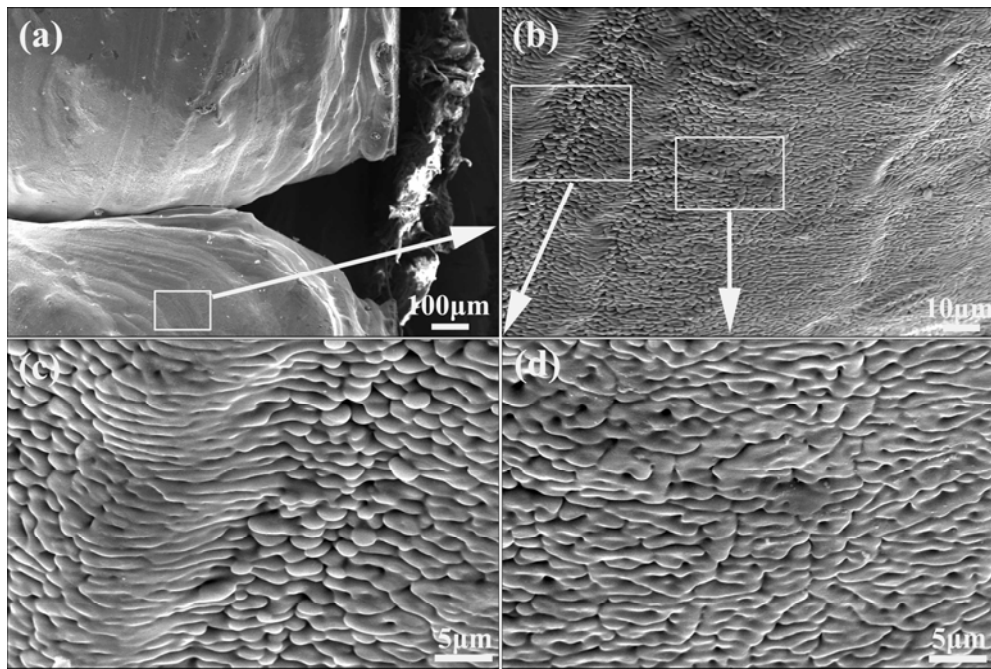


Fig. 8 SEM images of droplet surface in bottom region of two droplets overlap

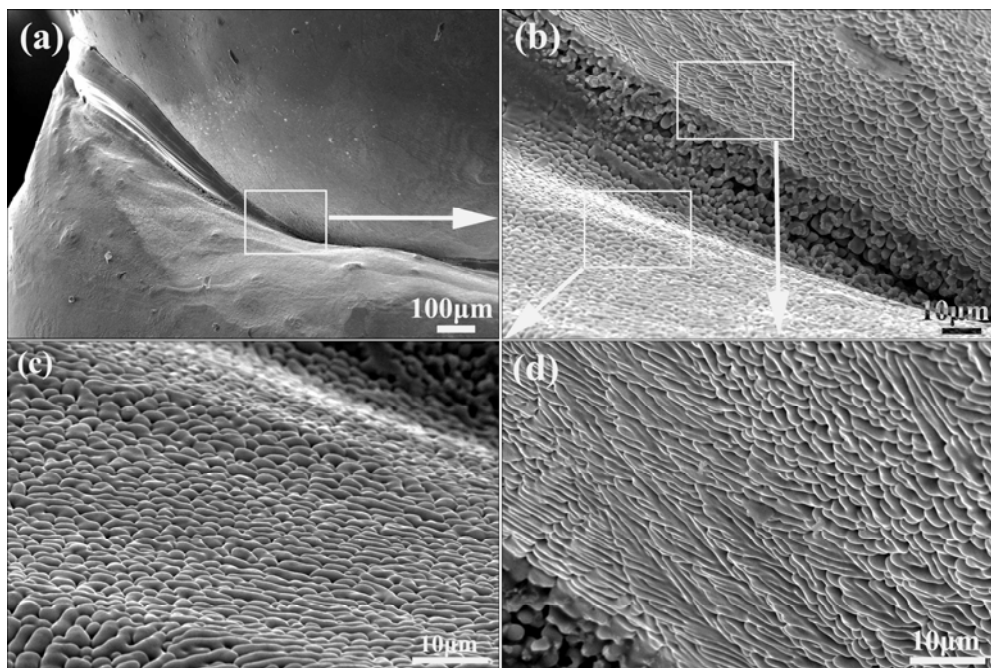


Fig. 9 SEM images of droplet surface in top region of two droplets overlap

2) The top temperature of droplets during the deposition varies with their orders, even is affected by overlap with the former droplet. The heat transferred from the high temperature droplet makes part of the solidified droplet in the contact area remelt, which favors to metallurgical bonding between droplets.

3) Predicated droplets shapes agreed well with SEM images of uniform molten 7075 Al alloy droplets onto a horizontally moving substrate under the same condition.

4) The effects of deposition and solidification of droplets result in vertical and L-shaped ridges on the

surface of droplets. Uniform tips of dendrites appear near the overlap of droplets due to rapid solidification, and scaly tips of dendrites appear due to remelting.

References

- [1] CIMA M, SACHS E, FAN T L, BRETT J F, MICHAELS S P, KHANUJA S, LAUDER A, LEE S J, BRANCAZIO D, CURODEAU A, TUERCK H. Three-dimensional printing techniques: US 5387380 [P]. 1993-04-20.
- [2] SACHS E, CIMA M, CORNIE J. Three-dimensional printing: rapid

- tooling and prototypes directly from a CAD model [J]. *CIRP Annals-Manufacturing Technology*, 1990, 39(1): 201–204.
- [3] KWACK W S, MOON H S, JEONG S J, WANG Q M, KWON S H. Hybrid functional IrO₂-TiO₂ thin film resistor prepared by atomic layer deposition for thermal inkjet printheads [J]. *Transactions of Nonferrous Metals Society of China*, 2011, 21(S): s88–s91.
- [4] MISHRA S, BARTON K L, ALLEYNE A G, FERREIRA P M, ROGERS J A. High-speed and drop-on-demand printing with a pulsed electrohydrodynamic jet [J]. *Journal of Micromechanics and Microengineering*, 2010, 20(9): 095026.
- [5] LUO Jun, QI Le-hua, LI Li, YANG Fang, JIANG Xiao-shan. Numerical simulation of jet breakup due to amplitude-modulated (A-M) disturbance [J]. *Transactions of Nonferrous Metals Society of China*, 2008, 18: 686–690.
- [6] TSENG A A, LEE M H, ZHAO B. Design and operation of a droplet deposition system for freeform fabrication of metal parts [J]. *Journal of Engineering Materials and Technology*, 2001, 123(1): 74–84.
- [7] QI Le-hua, CHAO Yan-pu, LUO Jun, ZHOU Ji-ming, HOU Xiang-hui, LI He-jun. A novel selection method of scanning step for fabricating metal components based on micro-droplet deposition manufacture [J]. *International Journal of Machine Tools and Manufacture*, 2012, 56: 50–58.
- [8] CHAO Yan-pu, QI Le-hua, XIAO Yuan, LUO Jun, ZHOU Ji-ming. Manufacturing of micro thin-walled metal parts by micro-droplet deposition [J]. *Journal of Materials Processing Technology*, 2012, 212(2): 484–491.
- [9] KANAI H, SUGUHARA S, YAMAGUCHI H, UCHIMARU T, OBATA N, KIKUCHI T, KIMURA F, ICHINOKURA M. Wetting and reaction between Si droplet and SiO₂ substrate [J]. *Journal of Materials Science*, 2007, 42(23): 9529–9535.
- [10] LIANG Gang-Tao, SHEN Sheng-qiang, GUO Ya-li, CHEN Jue-xian, YU Huan, LI Yi-qiao. Special phenomena of droplet impact on an inclined wetted surface with experimental observation [J]. *Acta Physica Sinica*, 2013, 62(8): 0847071.
- [11] CHEN Shi, WANG Hui, SHEN Sheng-qiang, LIANG Gang-tao. The drop oscillation model and the comparison with the numerical simulations [J]. *Acta Physica Sinica*, 2013, 62(20): 2047021–2047026.
- [12] LI Da-ming, WANG Zhi-chao, BAI Lin, WANG Xiao. Investigations on the process of droplet impact on an orifice plate [J]. *Acta Physica Sinica*, 2013, 62(19): 1947041.
- [13] TRAPAGA G, MATTHYS E F, VALENCIA J J, SZEKELY J. Fluid flow, heat transfer, and solidification of molten metal droplets impinging on substrates: Comparison of numerical and experimental results [J]. *Metallurgical and Materials Transactions B*, 1992, 23(6): 701–718.
- [14] KUMAR A, GHOSH S, DHINDAW B K. Simulation of cooling of liquid Al–33wt.% Cu droplet impinging on a metallic substrate and its experimental validation [J]. *Acta Materialia*, 2010, 58(1): 122–133.
- [15] LI He-jun, WANG Peng-yun, QI Le-hua, ZUO Han-song, ZHONG Song-yi, HOU Xiang-hui. 3D numerical simulation of successive deposition of uniform molten Al droplets on a moving substrate and experimental validation [J]. *Computational Materials Science*, 2012, 65: 291–301.
- [16] CAI Z B, ZHU M H, LIN X Z. Friction and wear of 7075 aluminum alloy induced by torsional fretting [J]. *Transactions of Nonferrous Metals Society of China*, 2010, 20(3): 371–376.
- [17] WILLIAMS J C, STARKE E A Jr. Progress in structural materials for aerospace systems [J]. *Acta Materialia*, 2003, 59(19): 5775–5799.
- [18] WANG Hui, LUO Ying-bing, PRIDEMAN P, CHEN Ming-he, GAO Lin. Warm forming behavior of high strength aluminum alloy 7075 [J]. *Transactions of Nonferrous Metals Society of China*, 2012, 22(1): 1–7.
- [19] SCHIAFFINO S, SONIN A A. Molten droplet deposition and solidification at low Weber numbers [J]. *Physics of Fluids*, 1997, 9: 3172–3187.
- [20] WALDVOGEL J M, POULIKAKOS D. Solidification phenomena in picoliter size solder droplet deposition on a composite substrate [J]. *International Journal of Heat and Mass Transfer*, 1997, 40(2): 295–309.

三维打印技术中 7075 铝合金 液滴沉积铺展过程的模拟

李海鹏¹, 李贺军¹, 齐乐华², 罗俊², 左寒松¹

1. 西北工业大学 凝固技术国家重点实验室, 西安 710072;

2. 西北工业大学 机电学院, 西安 710072

摘要: 采用基于流体体积法的三维模型研究按需喷射三维打印技术中均匀合金液滴的连续沉积和凝固过程。模型中使用的 7075 合金具有较大的相变温度范围。模拟结果表明: 该模型可以很好地模拟出 7075 合金均匀液滴的连续沉积和凝固过程, 模拟出的液滴形状和在相同条件下实验得出的 SEM 图像相吻合。液滴沉积和凝固的影响导致液滴表面出现垂直和“L”形的脊状突起, 液滴的快速凝固使搭接处出现细小的枝晶。

关键词: 7075 铝合金; 均匀液滴; 三维模型; 三维打印技术; 表面形貌

(Edited by Xiang-qun LI)